[265] The Impact of Different Precipitation Types on the Polarimetric Radar QPE Using Specific Attenuation in Taiwan

Yadong Wang*[1], Jian Zhang[2], Pengfei Zhang[3], Alexander Ryzhkov[3], Corwin Frittsh[1]

[1]Electrical and Computer Engineering Department,
Southern Illinois University Edwardsville, Edwardsville, IL

[2]Natioanl Severe Storms Laboratory, Norman, OK

[3]Cooperative Institute for Mesoscale Meteorological Studies,
University of Oklahoma, Norman, OK

ABSTRCT

The Quantitative Precipitation Estimation (QPE) algorithm using the specific attenuation ($R(A)$) has the advantages of immune to attenuation, radar miscalibration, wet radome, and partial beam blockage. Although the $R(A)$ algorithm is more robust to the variability of drop size distributions (DSD) compared to other radar rainfall relations, its performance could be further enhanced if the parameters in $R(A)$ approach could be automatically adjusted according to different precipitation types. This work investigates the impact of the precipitation types on $R(A)$ approach for both S-band and C-band polarimetric radar through simulation and real precipitation cases. For S-band polarimetric radar, the estimate of A from the ZPHI procedure requires tuning the net ratio $\alpha = A/K_{DP}$ along the radar beam. The coefficient α could be estimated based on the rain type and the slope of the Z–Z_{DR} dependency in a particular rain event. For C-band radar, the coefficient α is not sensitive to the precipitation types, but the R-A relationships for typical stratiform and convective could be significantly different. Adjusted $R(A)$ approaches for both C-, and S-band polarimetric radar located in Taiwan are proposed in this work. Their performances are evaluated using stratiform, convective, and typhoon precipitation events.

1. Introduction

A novel rainfall rate estimation approach using specific attenuation A was proposed by Ryzhkov et al. (2013). In this approach, the A field derived using the ZPHI method (e.g. Bringi et al. 1990, Testud et al. 2000) was suggested to be directly used in the rain rate estimation (Ryzhkov et al. 2014) as:

$$R = \gamma A^{\Lambda} \quad (1)$$

where coefficients γ and Λ depend on radar wavelength, temperature, and polarization. The units of R and A are mm hr^{-1} and dB km^{-1}, respectively. Using seven years drop size distribution (DSD) data set collected in Oklahoma, the $R(A)$ relations for different wavelengths (X-, C-, and S-bands) and polarizations (horizontal and vertical polarizations) were derived at temperatures of 0°C, 10°C, 20°C, and 30°C, respectively (Ryzhkov et al. 2013). The $R(A)$ approach is found immune to radar miscalibration, attenuation, partial beam blockage, and impact from wet radome. Applications of $R(A)$ relations for C-band and X-band polarimetric radars were also investigated by Wang et al. (2014), and Diederich et al. (2015), respectively. It was found that for a given DSD, both the factor α used in the A field estimation and γ in Equation 1 are temperature-dependent coefficients. However, the overall effect on α and γ has the trend of canceling each other, and the temperature effect can be ignored during the rainfall rate estimation (Wang et al. 2014). In the complex terrain, if the lowest tilt radar beam is blocked, the higher tilt A field needs be corrected from the vertical variations before implemented in the rainfall estimation (Wang et al. 2014).

It was found that $R(A)$ approach is less sensitive to the DSD variations than conventional $R(Z)$ and $R(Z,Z_{DR})$. However, more and more evidence indicates that the precipitation types (DSD) affect the $R(A)$ performance in the following two different aspects: 1.) S-band: factor α, a key parameter in the A field estimation, and 2.) C-band: R-A relationships.

This work investigates the impact of the precipitation types on the performance of $R(A)$ approach for S- and C-band polarimetric radar. This paper is organized as follows. In section 2, the impact of precipitation types

**Corresponding author address:* Yadong Wang, Electrical and Computer Engineering Department, Southern Illinois University Edwardsville, Edwardsville, IL.
e-mail: yadwang@siue.edu*

on S- and C-band is studied using simulation followed by the discussion of impact of hail in the *R*(*A*) approach in section 3. The performance evaluation is presented in section 4 with two cases, and summary and conclusion are given in section 5.

2. Method

2.1 The *R*(*A*) algorithm

In the *R*(*A*) approach (Ryzhkov et al. 2013), the *A* field is calculated using measured reflectivity Z_a and total span of ϕ_{DP} between ranges r_1 and r_2 as (Bringi et al. 1990, Testud et al. 2000, Ryzhkov et al. 2013):

$$A(r) = \frac{[Z_a(r)]^{\beta} C(\beta, PIA)}{I(r_1, r_2) + C(\beta, PIA) I(r, r_2)} \quad (2)$$

$$C(\beta, PIA) = \exp(0.23\beta PIA) - 1 \quad (3)$$

$$PIA(r_1, r_2) = \alpha[\phi_{DP}(r_2) - \phi_{DP}(r_1)] \quad (4)$$

where $I(r_1, r_2) = 0.46\beta \int_{r_1}^{r_2} [Z_a(s)]^{\beta} ds$, $I(r, r_2) = 0.46\beta \int_{r}^{r_2} [Z_a(s)]^{\beta} ds$, and $\beta = 0.62$. The radial profile of *A* is calculated between r_1 and r_2, where r_1 is the first gate contains precipitation, and r_2 is either the last precipitation gate or the gate right below the bottom of melting layer whichever is smaller. Significant bias on *A* field is resulted when the last gate r_2 is selected within or above melting layer.

For a S-band radar, the *R-A* relation in Equation 1 is less sensitive to the variations in the drop size distribution (DSD) than conventional *R-Z* and *R-Z-*Z_{DR} relations. For example, one set of γ and Λ ($\gamma = 4120$ and $\Lambda = 1.03$) can be applied on stratiform, convective and tropical precipitations at 20^{o}C for a S-band horizontal polarization radar (Ryzhkov et al. 2013)). On the other hand, the factor α in Equation 4 is the net ratio of *A* to K_{DP} along the ray, and it depends on temperature and is prone to DSD variability. It was found that the estimated α varies from 0.02 to 0.03 dB deg^{-1} over most areas of Hurricane Irene, and is within 0.008-0.015 dB deg^{-1} for the OKC flash flood case on 14 June 2010 (Ryzhkov et al. 2013). The value of α significantly effects the *A* field estimation, it will further determine the accuracy of the obtained rainfall rate. It was found that about 40% bias will result in the *R* field if the α decrease by 20% (Wang et al. 2014). More and more evidence indicates that α shows different values at different precipitation types. A real-time tuned α according to the DSD variability is expected to further enhance the performance of *R*(*A*) approach.

On the other hand, for a C-band radar, the α is stable for different precipitation type, but the *R-A* relation in Equation 1 is sensitive to the variations in the drop size distribution (DSD). Different *R-A* relations should be derived based on the precipitation types.

2.2 Simulation results

a.) S-band

Since the *A* field is determined by the factor α, which is highly related to the precipitation type, accurate *A* field could be calculated if the factor α could be real-time tuned according to the *Z-*Z_{DR} features. The relation between factor α and *Z-*Z_{DR} pair is studied through numerical simulation based on T-matrix method (Waterman 1971). In the simulation, the forward (backward) scattering amplitudes $f_{a,b}(0)$ ($f_{a,b}(\pi)$) of raindrops with diameters between 0.1 mm and 8 mm are first calculated at a temperature of 20^{o}C. Where *a* and *b* are the major and minor axes, respectively. The K_{DP}, *A*, *Z*, and Z_{DR} are calculated using formulas proposed by Zhang et al. (2001) with DSD data collected by four impact-type Joss-Waldvogel disdrometers (JWDs) located in Taiwan (Wang et al. 2014). There are total of 46,000 minutes of DSD data between April 2011 and June 2012 used in this work. The distribution of $\alpha = A/K_{DP}$ along Z_{DR}/Z is presented in Fig. 1 (A).

The nonlinear fitting results of $\alpha = 28.08\left(\frac{Z_{DR}}{Z}\right)^2 - 2.31\left(\frac{Z_{DR}}{Z}\right) + 0.0621$ is also inserted in Fig. 1 (A) as a reference. It could be found that the α decreases with the increase Z_{DR}/Z. The minimum α is approximate 0.01 dB deg^{-1}, and extremely large α presents when Z_{DR}/Z close to zero. Based on previous discussion, the small α is associated with small raindrops that are mainly from stratiform or tropical type precipiaiton, and the large α is mainly associated with convective type precipitation. For most of the cases, factor α varies between 0.01 to 0.035 dB deg^{-1}. It could be found that for a given observed *Z-*Z_{DR} data set, the most straightforward approach to estimate α is applying the derived polynomial, where calculating the Z_{DR}/Z is the mean ratio of all the data pairs. However, slight bias in either Z_{DR} or *Z* (such as caused by miscalibration) may significantly change the estimated α value, and the obtained *A* field may become very unstable.

An alternative approach to estimate α is using the *Z-*Z_{DR} slope *K*. The α-*K* relation in this work is derived using the same DSD data set, and is further divided into 300 periods with approximate 150-minute data in each time period. The precipitation type and DSD features in each period are assumed same. Following previous discussion, for each period, one α value could be calculated from the average ratio of K_{DP} and *A*, and one slope *K* could be obtained using linear fitting between the distribution of *Z* and Z_{DR}. The distribution of α-*K* is presented in Fig. 1 (B), and a linearly fitted line of $\alpha = -0.46K + 0.0423$ is included as a reference. Generally, the α shows decrease trend with the increase of *K*, and this is consistent with the result from Fig. 1 (A). In the current work, for S-band radar, the factor α is real-time calculated according to the slope of Z-Z_{DR}, and the A field is calculated using the adjusted α. The rainfall rate is estimated with fixed $R = 4120A^{1.03}$.

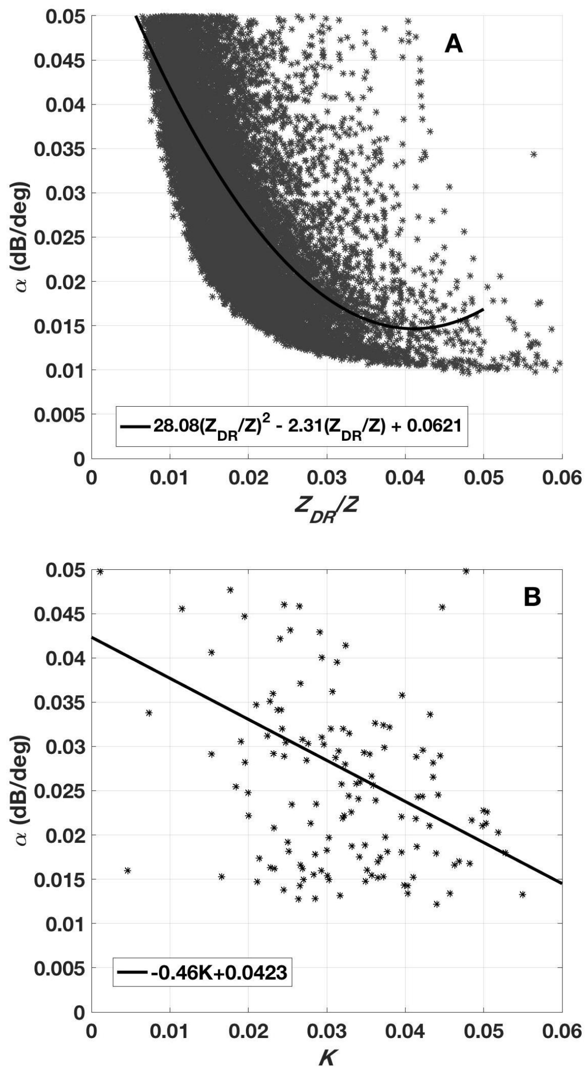

Figure 1. (A) the relation between factor α (dB/deg) and the ratio of Z and Z_{DR}. (B) The linearly fitted results.

b.) C-band

Using the same data set, the *R-A* relation for C-band polarimetric radar from different precipitation types are derived and shown in Fig 2. In this work, the DSD data is classified into stratiform, convective, and tropical precipitations. The *R-A* relations for each precipitation types are derived through the lease square fitting. It could be found that the *R-A* relations for stratiform and tropical types are very similar to each other, but significantly different from convective precipitation type. For the same *A* value, the stratiform and tropical relation can produce much more rainfall rate than convective precipitation. For the operational *R(A)* approach for C-band radar, the proper *R-A* relation from these derived three is selected according to the precipitation types (Zhang et al. 2016).

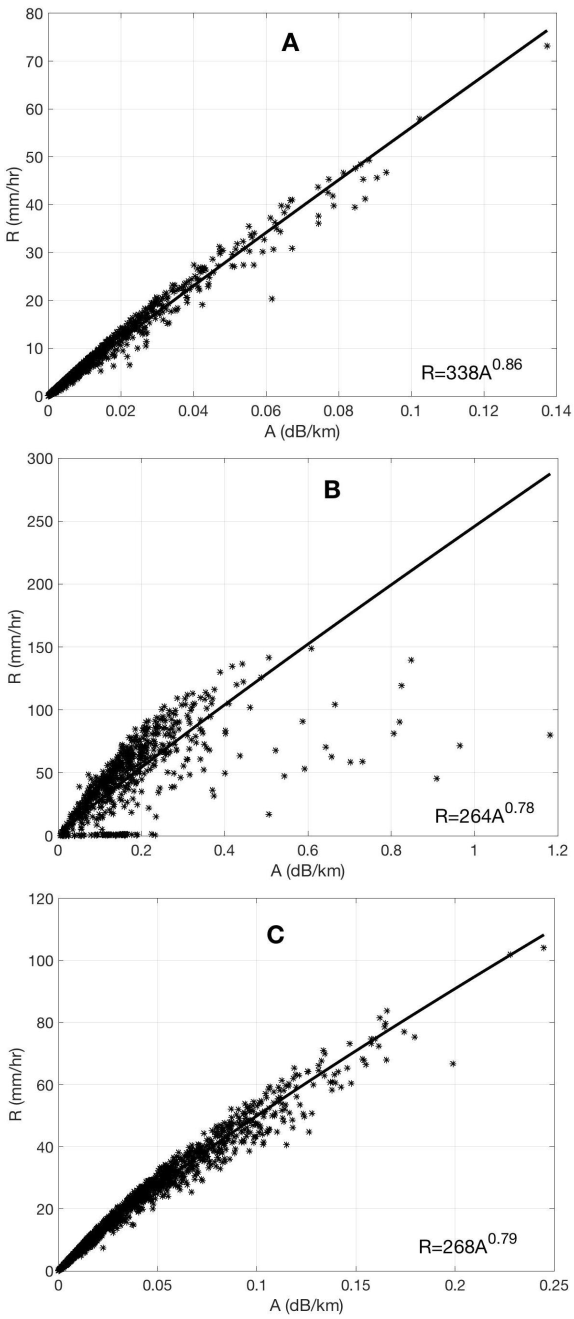

Figure 2. The relation between R-A for convective (A), tropical (B), and stratiform (C) precipitations.

3. The impact of hail in the *A* field estimation

Liquid phase medium (such as raindrops), whose relative dielectric constant is a specific value for a given temperature, is assumed in the A field estimation using Equations 1 ~ 3. The unique relation between Z, ϕ_{DP}, and A is established through the self-consistency principle when the DSD and drop shape relation (DSR) is specified. Under this assumption, the A could be estimated with path integrated Z and ϕ_{DP} using approach proposed by Ryzhkov et al. (2014). If mixed phase scatters (such as melted hail and wet snow) present in the radar resolution volume, the medium's dielectric constant becomes complicated, and is determined by many factors such as temperature, melting ratio, and etc. (Jung et al. 2007). The relation between Z, ϕ_{DP}, and A is not deterministic for a given DSD and DSR. Therefore, biased A will be resulted if the ϕ_{DP} and Z from the wet hail region are integrated in Equations 2 ~ 4.

An example is used in this work to demonstrate the A estimation when mixture of raindrop and wet hail presents in the radar propagation path. Fig. 3 presents the reflectivity field observed by KMOB at 0008 UTC 4 June 2014, and few regions of mixture of wet hail and raindrops with reflectivities above 55 dBZ could be identified from this example. A black line (azimuthal angle of 255.28°) indicates a radar beam going through one of the hail cores, where the hail region is between two black stars (r_3 = 33 km, and r_4 = 48 km). The r_1=13 km and r_2 = 85 km are the first and last gates in the integration as shown in Equations 1 and 3, where the last gate (r_2) is below the melting layer.

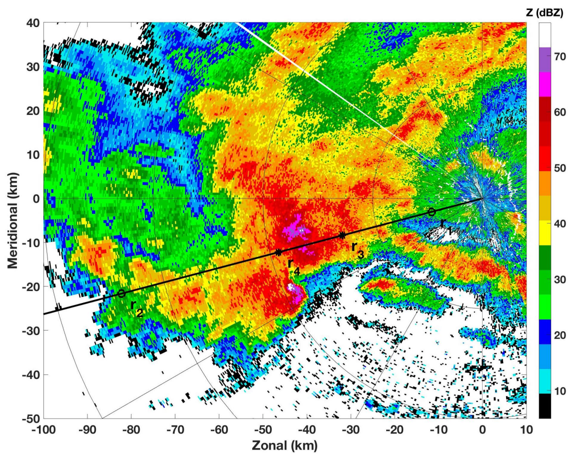

Figure 3: The reflectivity field at 0008 UTC 4 June 2014 observed by KMOB. The black line indicates the radar beam through hail region, where the hail region is between r_3 and r_4.

The profile of the Z and Z_{DR}, ϕ_{DP} and ρ_{HV} along this beam is presented in Fig. 5, respectively. It could be found in Fig. 4 (A) that the Z is above 55 dBZ between r_3 and r_4, and below 55 dBZ at r_1 ~ r_3 , and r_4 ~ r_2. The Z_{DR} shows significant fluctuations between r_3 and r_4, where values change from 1.2 dB to 4.0 dB. From r_3 to r_4, the ϕ_{DP} increases from 68.4° to 129° within 15 km, but the ϕ_{DP} only increase 13.0° within 21 km (r_1 ~ r_3) and 38.1° within 37 km (r_4 ~ r_2). The significant variations in the ϕ_{DP} field is caused by the mixture phased scatters in the radar beam propagation path. The ρ_{HV} between r_3 and r_4 are below 0.98, which is another indication of hail.

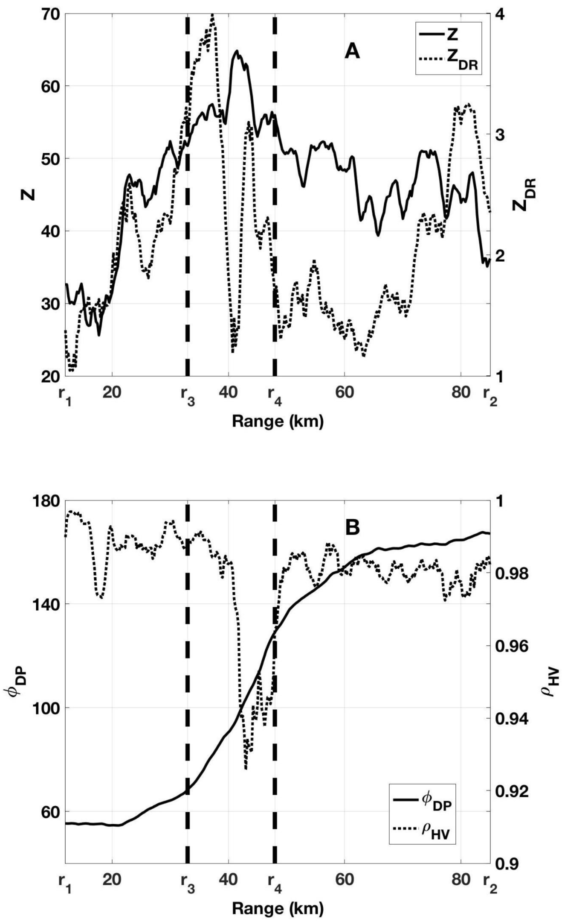

Figure 4: The profile of the Z and Z_{DR} (A), ϕ_{DP} and ρ_{HV} (B) along the black line in Fig. 3. The hail region is between r_3 and r_4.

In order to eliminate the contamination from hail in the A field estimation, the PIA and path integrated reflectivity is modified as:

$$PIA(r_1, r_2) = \alpha[(\phi_{DP}(r_2) - \phi_{DP}(r_1)) - (\phi_{DP}(r_4) - \phi_{DP}(r_3))] \quad (6)$$

$$I(r_1, r_2) = 0.46\beta\left(\int_{r_1}^{r_3}[Z_a(s)]^\beta ds + \int_{r_4}^{r_2}[Z_a(s)]^\beta ds\right) \quad (7)$$

When r is before r_3, $I(r, r_2) = 0.46\beta(\int_{r}^{r_3}[Z_a(s)]^\beta ds + \int_{r_4}^{r_2}[Z_a(s)]^\beta ds)$, and when r is after r_4 , $I(r, r_2) =$

$0.46\beta\int_{r}^{r_2}[Z_a(s)]^{\beta}ds$. Using the modified equation, A field is only calculated in the rain region ($r_1 \sim r_3$ and $r_4 \sim r_2$), and no A is calculated in the hail region ($r_3 \sim r_4$). The A profile estimated using modified approach is shown in Fig. 4 (B) with solid line (A_2). It should be noted that A_2 is lower than A_1 in the rain regions ($r_1 \sim r_3$ and $r_4 \sim r_2$). This because anomalous increases in Z and ϕ_{DP} caused by hail are distributed into each gate in the integration path. Therefore, the estimated whole radial A is biased if those gates from hail region are not excluded from the integration.

4. Performance Evaluation

Two 24-hour precipitation events are used to evaluate the performance of upgraded $R(A)$ approach for S- and C-band polarimetric radar. In the evaluation, the rainfall rate is estimated, and then compared with gauge network observations. Three scores were used to assess the QPE performance: 1) mean bias: $B = \langle R_p\rangle/\langle G_p\rangle$, 2) root-mean-square error: $R = \langle(G_p - R_p)^2\rangle^{1/2}$, and 3) correlation coefficient: $C = \langle(R_p - \langle R_p\rangle)(G_p - \langle G_p\rangle)\rangle/\sigma_R\sigma_G$, where angle brackets indicate the mean of the samples, R_p and G_p are the 24-hour radar and gauge accumulated rainfall for each pair p, and σ_R (σ_G) is the standard deviation of all the radar (gauge) pairs. It should be noted that all gauges used in the current work are quality controlled, and those gauges show apparent biases are removed from the evaluation.

4. 1 S-band polarimetric radar

The performance of the modified $R(A)$ approach is tested on RCWF using 24-hour data (0000~2400 UTC) at 04/20/2015. In this approach, the α is real-time estimated using Z-Z_{DR} slope, and the A field is estimated using the adjusted α. The 24 hours accumulation is shown in Fig 5. Because of the severe radar beam blockage (within the red circle), data from higher than 0.5-degree elevation angle is used in the rainfall rate estimation (within the white circle).

The comparison result between radar QPE and gauge observation is shown in Fig. 6. The size of the bubble in Fig. 6 (a) indicates the 24-hour accumulation observed by gauges, and the color indicates the mean ratio between radar QPE and gauge measurements, where warm colors (pink to red) and cold colors (light blue to dark blue) represent underestimation and overestimation, respectively. For this case, the upgraded R(A) approach can produce mean bias of 0.93, correlation coefficient of 0.78, and mean square root error of 9.39 mm.

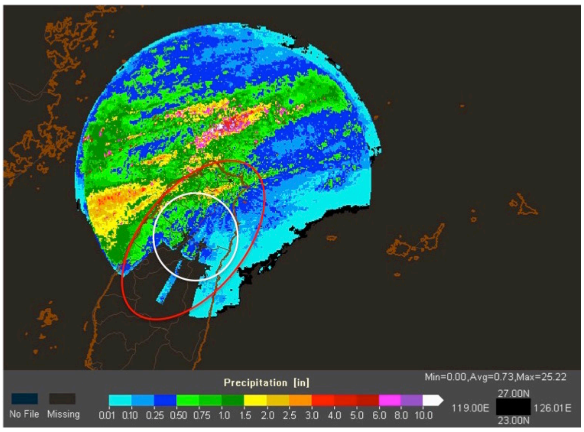

Figure 5, The 24-hour accumulated rainfall (0000~2400 UTC 04/20/2015) using updated $R(A)$ approach for a S-band polarimetric radar RCWF.

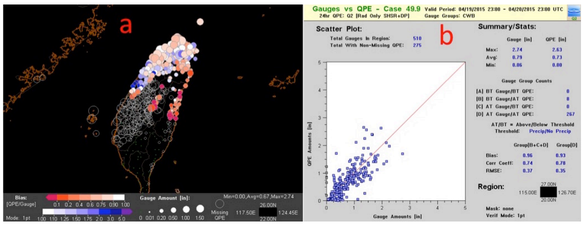

Figure 6, The 24-hour radar QPE is compared with gauge observations, and the comparison is shown in Fig. 5. The mean bias is 0.93, correlation coefficient is 0.78 and root mean square root error is 0.35 in (9.39 mm).

4. 2 C-band polarimetric radar

The performance of the modified $R(A)$ approach on one C-band dual-polarization radar (RCMK) is evaluated with 24 hours precipitation event on 0000 ~ 2400 UTC 09/28/2015 (Typhoon Dujuan). In this approach, the R-A relations are real-time adjusted according to the precipitation types (Zhang et al. 2016). The 24-hours QPE accumulation is shown in Fig. 7, and the comparison result in shown in Fig. 8. For this case, the radar QPE can produce really good results in terms of 1.13 mean bias, 0.83 correlation coefficient and 53.24 mm root mean square root error.

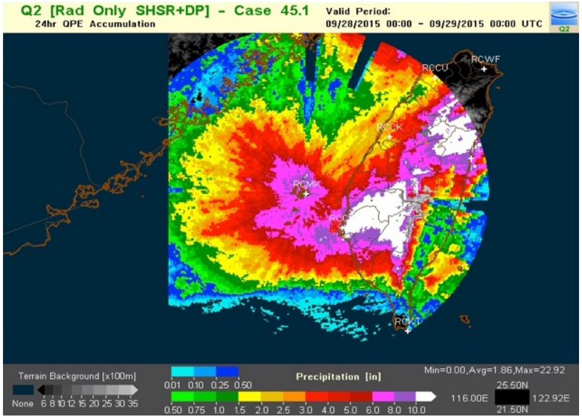

Figure 7, The 24-hour accumulated rainfall (0000~2400 UTC 09/28/2015) using updated $R(A)$ approach for a C-band polarimetric radar RCMK.

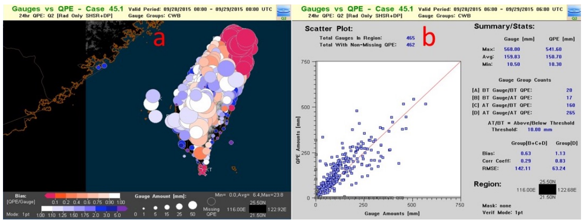

Figure 8, The 24-hour radar QPE is compared with gauge observations, and the comparison is shown in Fig. 7. The mean bias is 1.13, correlation coefficient is 0.83 and root mean square root error is 53.24 mm.

5. Summary

The original quantitative precipitation estimation (QPE) approach using specific attenuation ($R(A)$) was found immune to radar miscalibration, attenuation, partial beam blockage, and impact from wet radome. Although the $R(A)$ approach is less sensitive to the DSD variations than conventional $R(Z)$ and $R(Z, Z_{DR})$ approaches, more and more evidence show that the impacts of the precipitation types (DSD) on $R(A)$ can be significant, and need to be considered when apply the $R(A)$ approach in the real-time QPE.

To mitigate the impact of precipitation properties variations on the A field estimation and further enhance the performance of $R(A)$ approach, operational S-band $R(A)$ approach for S-band and C-band polarimetric radars were proposed in the current work. For S-band radar, the A field is estimated with a real-time adjusted α, which is calculated from the slope of the Z-Z_{DR} pairs. The relation between the Z-Z_{DR} slope and α is obtained through the T-matrix method with observed DSD data. The slope can capture the DSD features from different precipitation categories, and also is not affected by the absolute calibration. For C-band radar, the R-A relations for different precipitation types are investigated through simulation. In this work, the precipitation is first classified into stratiform, convective and tropical, and the R-A relations are then derived through least square fitting. This work also investigates the impact of the hail in the $R(A)$ approach, and suggests a modified integration approach that exclude the hail region from the integration path. With these upgrades, the modified R(A) can produce good QPE results for both S- and C-band polarimetric radars.

6. Acknowledgement

Part of this work is supported by the undergraduate research and creative activities (URCA) program from Southern Illinois University Edwardsville.

7. References

Diederich M., A. V. Ryzhkov, C. Simmer, P. Zhang, and S. Tromel, 2015: Use of specific attenuation for rainfall measurement at X-band radar wavelengths. Part II: Rainfall estimation and comparison with rain gauges. *J. of Hydrometeorology*, **16**, 503-516.

Giangrande, S., and A. Ryzhkov, 2008: Estimation of rainfall based on the results of polarimetric echo classification. *J. Appl. Meteor.*, **47**, 2445-2462.

Gorgucci E., G. Scarchilli, and V. Chandrasekar, 1993: A robust estimator of rainfall rate using differential reflectivity. *J. Atmos. Oceanic Technol.,* **11**, 586-592.

Gourley J. J., A. J. Illingworth, and P. Tabary, 2009: Absolute calibration of radar reflectivity using redundancy of the polarization observations and implied constraints on drop shapes. *J. Atmos. Oceanic Technol.,* **26**, 689-6703.

Jung Y., G. Zhang, and M. Xue, 2007: Assimilation of simulated polarimetric radar data for a convective storm using the ensemble kalman filter. Part I: observation operators for reflectivity and polarmetric variables. *Monthly Weather Review*. **136**, 2228-2245.

Park, S.-G., V. Bringi, V. Chandrasekar, M. Kaki, and K. Iwanami, 2005: Correction of radar reflectivity and differential reflectivity for rain attenuation at X band. Part II: evaluation and application. *J. Atmos. Oceanic Technol.,* **22**, 1633-1655.

Tang, L., J. Zhang, C. Langston, J. Krause, K. Howard, and V. Lakshmanan, 2014: A physically based precipitation-nonprecipitation radar echo classifier using polarimetric and environmental data in a real-time national system. *Wea. Forecasting*, **29**, 1106-1118

Ryzhkov, A., and D. S. Zrnic, 1995: Comparison of dual-polarization radar estimators of rain. *J. Atmos. Oceanic Technol.*, **12**, 249-256.

Ryzhkov, A., M. Diederich, P. Zhang, and C. Simmer, 2014: Potential utilization of specific attenuation for rainfall estimation, mitigation of partial beam blockage, and radar networking. *J. Atmos. Oceanic Technol.,* **31**, 599-619.

Seliga, T. A., and V. N. Bringi, 1976: Potential use of the radar reflectivity and orthogonal polarizations for measuring precipitation. *J. Appl. Meteor.*, **15**, 69-76.

Testud, J., E. Le Bouar, E. Obligis, and M. Ali-Mehenni, 2000: The rain profiling algorithm applied to polarimetric weather radar. *J. Atmos. Oceanic Technol.*, **17**, 332-356.

Vulpiani, G., M. Montopoli, L. Delli Passeri, A. Giola, P. Giordano, and F. Marzano, 2012: On the use of dual-polarized C-band radar for operational rainfall retrieval in mountainous area. *J. Appl. Meteor. Climatol.*, **51**, 405-425.

Wang, Y., J. Zhang, A. V. Ryzhkov, and L. Tang, 2013: C-band polarimetric radar QPEs based on specific differential propagation phase for extreme typhoon rainfall. *J. Atmos. Oceanic Technol.*, **30**, 1354-1370.

Wang, Y., J. Zhang, P.-L. Chang, C. Langston, B. Kaney, and L. Tang, 2016: Operational C-band dual-polarization radar QPE fort the subtropical complex terrain of Taiwan. *Advances in Meteorology,* **2016** 1-15. http://dx.doi.org/10.1155/2016/4294271

Wang, Y., P. Zhang, A. V. Ryzhkov, J. Zhang, and P.-L. Chang, 2014: Utilization of specific attenuation for tropical rainfall estimation in complex terrain. *J. of Hydrometeorology*, **15**, 2250-2266.

Waterman, P. C., 1971: Symmetry, unitarity and geometry in electromagnetic scattering. *Phys. Rev. D*, **3**, 825-839, doi: 10.1103/PhysRevD.3.825

Zhang, G., J. Viekanandan, and E. Brandes, 2001: A method for estimating rain rate and drop size distribution from polarimetric radar measurements. *IEEE Trans. Geosci. Remote Sens.*, **39**, 830-841, doi: 10.1109/36.917906.

Zhang, J., and Coauthors, 2016: Multi-radar multi-sensor (MRMS) quantitative precipitation estimation: initial operating capabilities. *Bull. Amer. Meteor. Soc.*, **97**, 621-638, doi:10.1175/BAMS-D-14-00174.1